Jurnal Sainstech Nusantara	Vol. 2 No. 1 (2025) 38-52
https://nusantarajournal.id/sainstech	ISSN: 3063-0657

The Effect of Triangular Vortex Generator Straight Arrangements on the NACA 0012 Airfoil Using a Smoke Generator

Saniyya Nahda Trysnavirensa[1], Setyo Hariyadi Suranto Putro[1], Nyaris Pambudiyatno[1]

[1]Department of Aircraft Maintenance Engineering, Politeknik Penerbangan Surabaya, Jl. Jemur Andayani I/73, Surabaya 60236, INDONESIA

Article Info

Article history:

Received 26 December, 2024
Revised 9 January, 2025
Accepted 12 February, 2025

Abstract

Aerodynamics is a fundamental discipline in the field of aviation, as it governs the airflow around an aircraft, enabling lift generation. The design and construction of aircraft wings are critical, as they directly impact the aircraft's stability and lift efficiency. Thus, aerodynamics plays a pivotal role in the performance, functionality, and overall design of aircraft. With advancements in modern aviation, continuous improvements are being made in the design and configuration of wing models. To analyze the aerodynamic characteristics of an aircraft wing, the airflow distribution method is commonly employed, one of which includes the use of vortex generators. This study investigates the effects of adding triangular vortex generators to a NACA 0012 airfoil, utilizing the smoke generator method in a straight arrangement. The experiments were conducted in an open-circuit wind tunnel with an airflow velocity of 5 m/s. The angles of attack tested were 0°, 4°, 8°, 10°, 15°, 17°, and 20°. The vortex generators were positioned 20% of the chord length from the leading edge of the airfoil. The experimental results demonstrate that the addition of triangular vortex generators increases the distance to the furthest point of separation and enhances the transition point on the airfoil. The aerodynamic performance of the airfoil was evaluated based on the observed airflow patterns around the airfoil, which showed notable differences compared to the airfoil without vortex generators.

Keywords: Vortex generator, Smoke generator, Wind tunnel, NACA 0012 airfoil

Corresponding Author:

Name: Saniyya Nahda Trysnavirensa
Email: rensa.nahda@gmail.com

1. Introduction

Aerodynamics is a core discipline within fluid dynamics, focusing on the study of air movement around objects, particularly in the context of aviation. The term “aerodynamics” is derived from two

DOI: https://doi.org/10.71225/jstn.v2i1.86

Greek roots: “aero,” meaning air, and “dynamics,” which refers to the forces or motions acting on moving objects [1]. In the field of aviation, aerodynamics plays a vital role in shaping the performance, design, and overall efficiency of aircraft. Understanding the interaction between air and various surfaces of an aircraft is crucial for optimizing flight performance, safety, and fuel efficiency. The study of aerodynamics extends beyond basic fluid dynamics principles to their practical applications in aircraft systems. A key element of aerodynamics is how airflow influences the forces acting on an aircraft, notably lift, drag, thrust, and weight. Among these forces, lift is the most critical, as it directly sustains the aircraft’s flight [2] [3] [4].

Lift is generated by the pressure difference between the upper and lower surfaces of an airfoil. Airflow over the airfoil can be categorized into two types: laminar and turbulent flow. Laminar flow is smooth and orderly, whereas turbulent flow, often referred to as wake, is characterized by chaotic eddies and vortices, which can significantly affect the aerodynamic performance of an aircraft. A major challenge for aerodynamicists is managing this turbulent flow to maintain efficient and steady airflow over the airfoil [5] [6]. To address this challenge, various strategies, such as the use of vortex generators, are employed. Vortex generators are small aerodynamic devices designed to enhance airflow characteristics over an airfoil. These devices create controlled turbulence within the boundary layer, thereby delaying flow separation and reducing drag. The introduction of vortex generators (VGs) has been shown to improve aerodynamic efficiency by maintaining smoother airflow over the airfoil, which leads to a better lift-to-drag ratio and overall improved performance. Vortex generators are often tested in wind tunnels, allowing for precise measurements of their effect on airflow and aerodynamic behavior [7] [8].

Recent research in aerodynamics has highlighted the potential benefits of vortex generators in improving airfoil performance. Pradana (2019) investigated the impact of vortex generators on airfoils with fixed-wing designs, employing flow visualization techniques to analyze boundary layer characteristics [9]. This experimental setup provided valuable insights into the effects of vortex generators on pressure distribution, drag coefficients (CD), and lift coefficients (CL). Similarly, Pratama (2021) examined the impact of rectangular vortex generators on the NACA 0012 airfoil using a counter-rotating configuration. The findings from these studies underscore the importance of vortex generator placement and arrangement in optimizing aerodynamic characteristics. Both studies employed wind tunnel testing as a method for observing changes in airflow over the airfoil, which emphasizes the need for accurate measurement and control in experimental setups [10] [11].

Despite the significant body of research on vortex generators, the design and placement of these devices remain subjects of ongoing investigation. Much of the existing research has primarily focused on rectangular vortex generators, offering valuable insights into airflow improvement. However, there is a growing need to explore alternative vortex generator designs, such as triangular vortex generators, to better understand their comparative performance. The current literature does not sufficiently address the performance of triangular vortex generators in comparison to other designs, especially concerning their effects on airflow separation and lift-to-drag ratios [13] [14]. Given the wide variety of vortex generator configurations, it is necessary to explore the performance of triangular vortex generators through wind tunnel experiments to fill this gap in knowledge [15].

The primary research problem emerging from this gap in the literature is the need to analyze the specific effects of triangular vortex generators on the flow characteristics of airfoils. This study aims to address the following research questions: (1) How does a triangular vortex generator affect the airflow over the surface of an airfoil? (2) How does the fluid flow differ between an airfoil with a triangular vortex generator and one without? (3) How does the presence of a vortex generator influence the flow separation point compared to an airfoil without a vortex generator. These questions

DOI: https://doi.org/10.71225/jstn.v2i1.86

are essential for determining the impact of triangular vortex generators on aerodynamic performance, with potential implications for aircraft design and efficiency [16] [17].

To explore these issues, this study will utilize an open-circuit wind tunnel, a commonly used tool in aerodynamics experiments due to its simplicity and effectiveness in providing accurate airflow measurements. The wind tunnel will allow for precise observation of the effects of vortex generators on airfoil behavior under controlled conditions. The study will focus on the NACA 0012 airfoil, a well-established aerodynamic profile widely used in experimental studies. By employing smoke visualization to track the flow over the airfoil, this research will examine the differences in fluid dynamics when a triangular vortex generator is added compared to an airfoil without any vortex generator [18] [19].

While previous studies have demonstrated the positive effects of vortex generators on airfoil performance, limited research has been conducted on the use of triangular vortex generators. Hariyadi (2018) investigated the impact of rectangular vortex generators on airflow around airfoils, but did not explore triangular vortex generators as an alternative. Therefore, this research seeks to address this gap by examining the specific impact of triangular vortex generators on aerodynamic performance using the NACA 0012 airfoil as the test model [20] [21]. This study will provide a more comprehensive understanding of vortex generator designs and their applications in aircraft aerodynamics, contributing valuable insights to the optimization of wing performance.

The objective of this research is to investigate the operating principles of triangular vortex generators, analyze their effect on airflow over an airfoil, and assess how their application influences the flow separation point. The findings from this study will provide new insights into the efficiency of triangular vortex generators in improving lift and reducing drag on airfoils. Specifically, this research aims to determine whether triangular vortex generators offer superior aerodynamic performance compared to other vortex generator designs. In doing so, it will enhance our understanding of the role of vortex generators in improving the overall aerodynamic efficiency of aircraft. In conclusion, this study aims to address a significant gap in the current literature by exploring the effects of triangular vortex generators on aerodynamic performance. The results of this research are expected to contribute to the broader field of aerodynamics and offer practical recommendations for aircraft design, potentially leading to more efficient and cost-effective aviation solutions. The use of triangular vortex generators could provide an innovative approach to optimizing airfoil performance, improving the understanding of airflow dynamics, and offering insights that could be applied to both commercial and military aircraft designs.

2. Materials and Method

This section outlines the experimental method employed in this study, utilizing a wind tunnel simulation. The test subject for this experiment is the NACA 0012 airfoil, placed in a wind tunnel with controlled airflow. The geometry of both the aerodynamic surface and the wind tunnel was designed with a length of 1 x 10.5 meters to ensure valid and accurate results.

2.1 Experimental Design

The model used for the wing test is the NACA 0012 airfoil. No modifications are made to the airfoil to investigate the effects of airflow over the upper surface, focusing on the angle of attack, lift, and drag characteristics [10].

DOI: https://doi.org/10.71225/jstn.v2i1.86

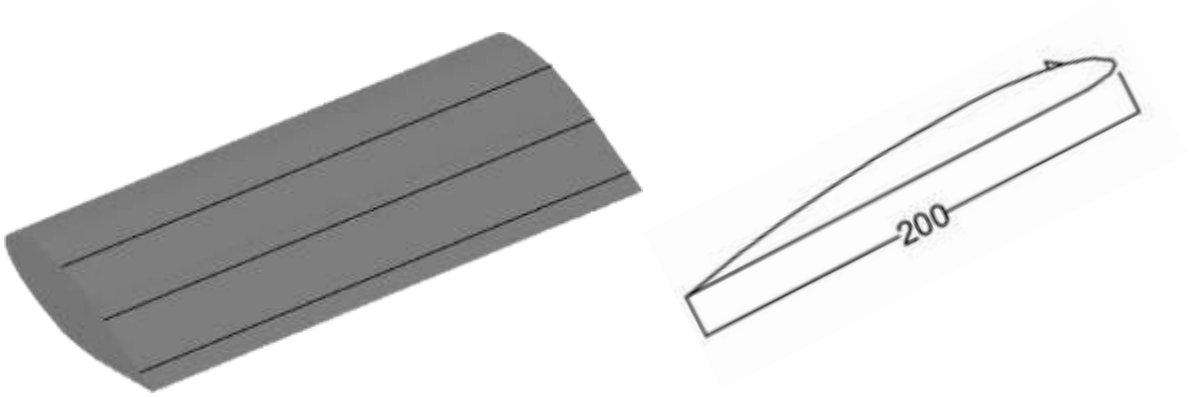

Figure 1. Airfoil Naca 0012

Table 1. Dimensional analysis is conducted to determine which parameters affect the experiment

Fluid density	*p (kg/m3)*
Fluid velocity	*U∞ (m/s)*
Boundary layer thickness	*(m)*
Airfoil thickness	*x (m)*
Distance between the flat plate wall and the airfoil	*G (m)*
Airfoil chord length	*c (m)*
Vortex generator height	*h(m)*
Vortex generator length	*l(m)*
Distance from leading edge to vortex generator	*t(m)*

Table 2. The vortex generator parameters used in this study

Parameter	**Experiment**
Shape	Tringular
H	0.00086.C
1/H	3
Aoa	0˚,4˚,8˚,10˚,15˚,17˚dan 20˚
X/C	20%
C	200 Mm
D	0,182.C
Arrangement	Straight
V	5 M/S

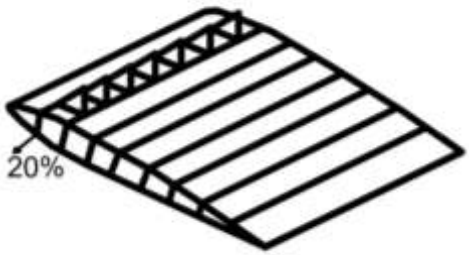

Figure 2. Placement of Triangular Vortex Generator 3 Dimensions

DOI: https://doi.org/10.71225/jstn.v2i1.86

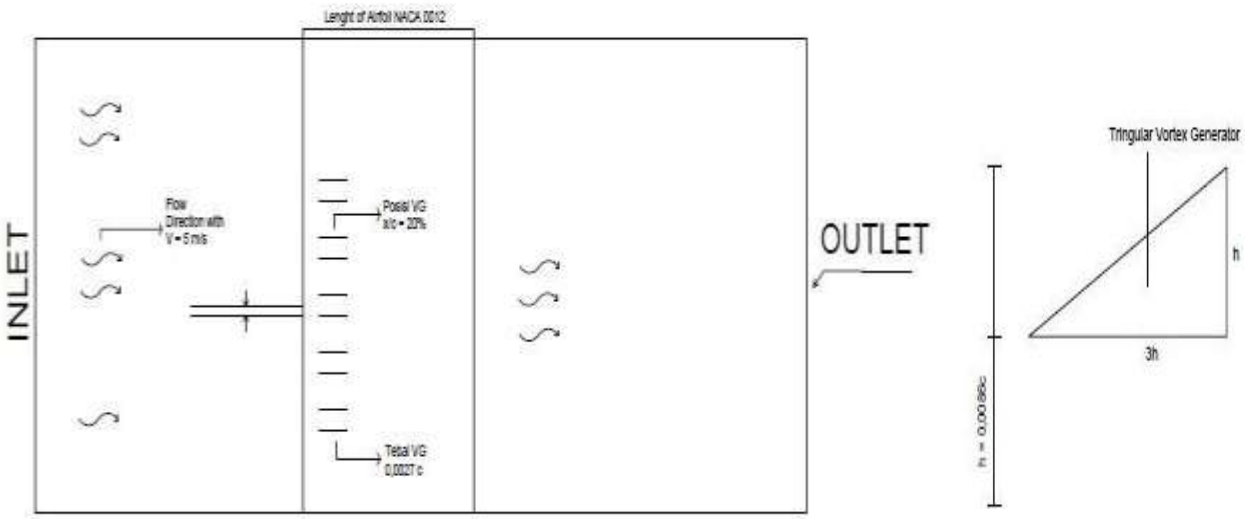

Figure 3. Vortex Generator Parameter

2.2 Experimental test

In this study, an open-circuit wind tunnel with a speed of 5 m/s is used to test the model at scale. Air is drawn from the surrounding environment, passed through a venturi-shaped tube, and then released into the open air. This setup simulates realistic conditions, and the results are expected to be accurate. The wind tunnel is of the open circuit type, designed for subsonic flow. The test section has the following dimensions: a length of 180 cm and a height of 66 cm. The wind tunnel operates under subsonic conditions, where the flow velocity is less than Mach 1.0. Mach is a velocity unit representing the speed relative to the speed of sound, which is approximately 331.6 m/s in air at sea level under standard conditions. Subsonic: Mach < 1.0, Sonic: Mach = 1.0, Transonic: 0.9 < Mach < 1.0 and Hypersonic: Mach > 5.0 [10] [12].

Figure 4. Wind tunnel

The initial step in the preparation phase involves conducting a comprehensive inspection to ensure that all equipment is properly installed according to its designated placement and function. This inspection should extend to the inlet area of the wind tunnel to verify that no air leaks are

DOI: https://doi.org/10.71225/jstn.v2i1.86

present. Once the equipment is confirmed to be in optimal condition, the necessary tools and materials for the experiment should be gathered. Following this, it is essential to verify that the test object is correctly installed and securely positioned within the test section. Visual data collection is performed using a 12 MP camera equipped with 100% Focus Pixels (Wide), Deep Fusion, Smart HDR 3, and automatic image stabilization. The camera operates in burst mode to ensure accurate image capture. During model installation, ensure that the NACA 0012 airfoil is correctly placed in the test section with the vortex generator (VG) component securely attached. It is crucial to check that the airfoil is properly balanced, free from air leaks, and that the fogging machine is prepared for use prior to initiating the test.

In the run phase, the axial fan motor is activated, and the airflow is adjusted to reach the desired airspeed of 5 m/s. This adjustment is made by controlling the freestream via the PC monitor and inverter until the required airspeed is achieved. Subsequently, data is collected by observing the smoke characteristics on the upper surface of the airfoil. The camera captures these smoke flow patterns. Once the data collection is complete, the airflow is stopped, the speed is set to 0 m/s, and the fan is turned off. Finally, the electrical supply to the wind tunnel is disconnected.

For data retrieval, tools such as tape, scissors, and a ruler are used to outline the airfoil and attach the vortex generator (VG) at a position located 20% of the chord length (x/c = 20%) or 40 mm from the leading edge. Side-angle images are taken to visualize the smoke flow passing over the airfoil. If necessary, the imaging process is repeated to ensure optimal results [10] [12].

The data analysis in this study follows a quantitative approach, where numerical data obtained from the images are compiled and analyzed to support scientific findings. The collected data is categorized into discrete and continuous types. Discrete data, or nominal data, is derived from observation or experience, while continuous data, which includes ordinal, interval, and ratio data, is derived from measurements. Ordinal data provides a scale within the study, while interval data pertains to measurements made at consistent points with the same distance. This research, supported by the NACA 0012 airfoil and smoke visualization, aims to generate comprehensible results that will fulfill the research objectives of the final project [16].

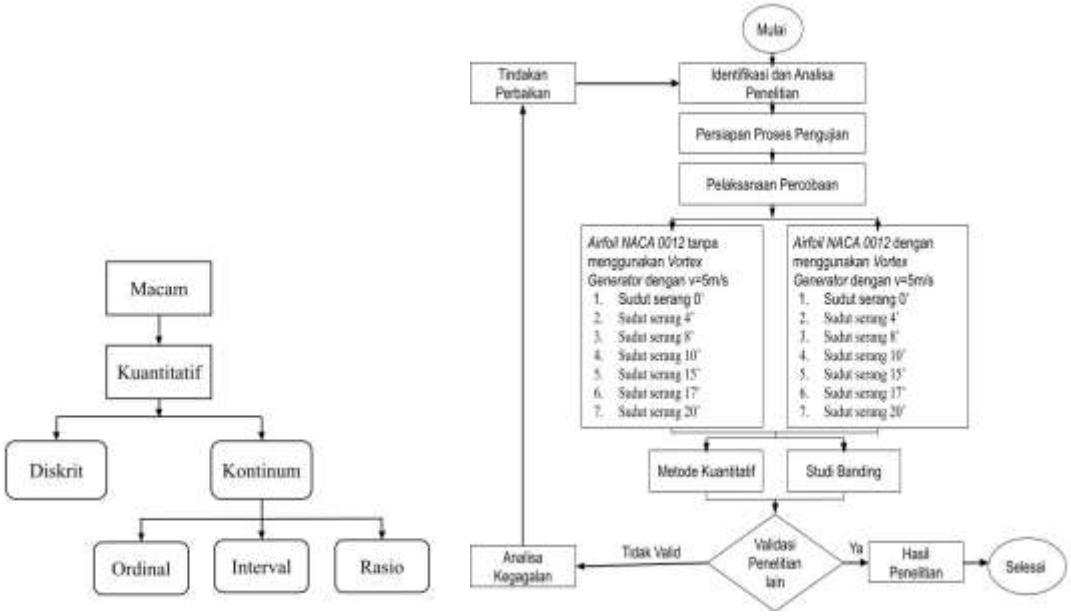

Figure 5. (a) Research Data (b) Fwowchart test procedure

DOI: https://doi.org/10.71225/jstn.v2i1.86

3. Results and Discussions

3.1 Flow Transition, Separation, and Vorticity Analysis

This section presents and discusses the research findings obtained after conducting the experiment. The test was performed using the smoke visualization technique on the NACA 0012 airfoil, equipped with a triangular vortex generator in a straight configuration. The wind tunnel test was conducted at a velocity of 5 m/s, with variations in the angle of attack set to 0°, 4°, 8°, 10°, 15°, 17°, and 20°. The results are documented through photographic evidence. The findings of this study indicate that the introduction of a vortex generator on the airfoil significantly affects the airflow over the upper surface of the wing. This effect varies according to the angle of attack. The vortex generator increases the transition length from laminar to turbulent flow, and the separation point shifts towards the trailing edge of the airfoil. The smoke generator was damaged and failed to produce smoke during the experiment. Several factors contributed to this failure, including improper usage during the previous test and a blocked smoke-producing tube. To resolve this issue, a fogging machine was used as an alternative, though additional modifications were made to ensure the smoke was directed through a single outlet, mimicking the original smoke generator's functionality. However, the flow of smoke could not be controlled, and the visualization process was complicated by inconsistent smoke output. Consequently, repeated visualizations were necessary to clearly identify the separation flow and achieve reliable results. The smoke flow patterns in the NACA 0012 airfoil differed significantly with and without the vortex generator. In the absence of the vortex generator, the smoke flow initially strikes the leading edge but fails to follow the airfoil's contour, resulting in undirected flow. In contrast, when a triangular vortex generator was added, the smoke flow followed the shape of the airfoil and was directed towards the trailing edge. Based on the experimental results, transition points (Xl), separation points (Xs), and vortex points (Xt) were identified and tabulated. Transition Point: The point at which laminar flow transitions to turbulent flow. Separation Point: The location where the airflow detaches from the surface due to an adverse pressure gradient. Vorticity Point: The point where the airflow begins to rotate, contributing to vortex formation.

Table 3. Plain Airfoil

α	Xl	Xs	Xt
0˚	0.1	0.7	0.8
4˚	0.18	0.68	0.77
8˚	0.15	0.62	0.7
10˚	0.15	0.6	0.8
15˚	0.1	0.4	0.6
17˚	0.13	0.28	0.4
20˚	0.12	0.2	0.3

Table 4. Triangular Vortex Generator

α	Xl	Xs	Xt
0˚	0.2	0.76	0.85
4˚	0.23	0.8	0.9
8˚	0.2	0.8	0.9
10˚	0.19	0.8	0.89
15˚	0.2	0.65	0.7

DOI: https://doi.org/10.71225/jstn.v2i1.86

17˚	0.18	0.5	0.7
20˚	0.15	0.45	0.5

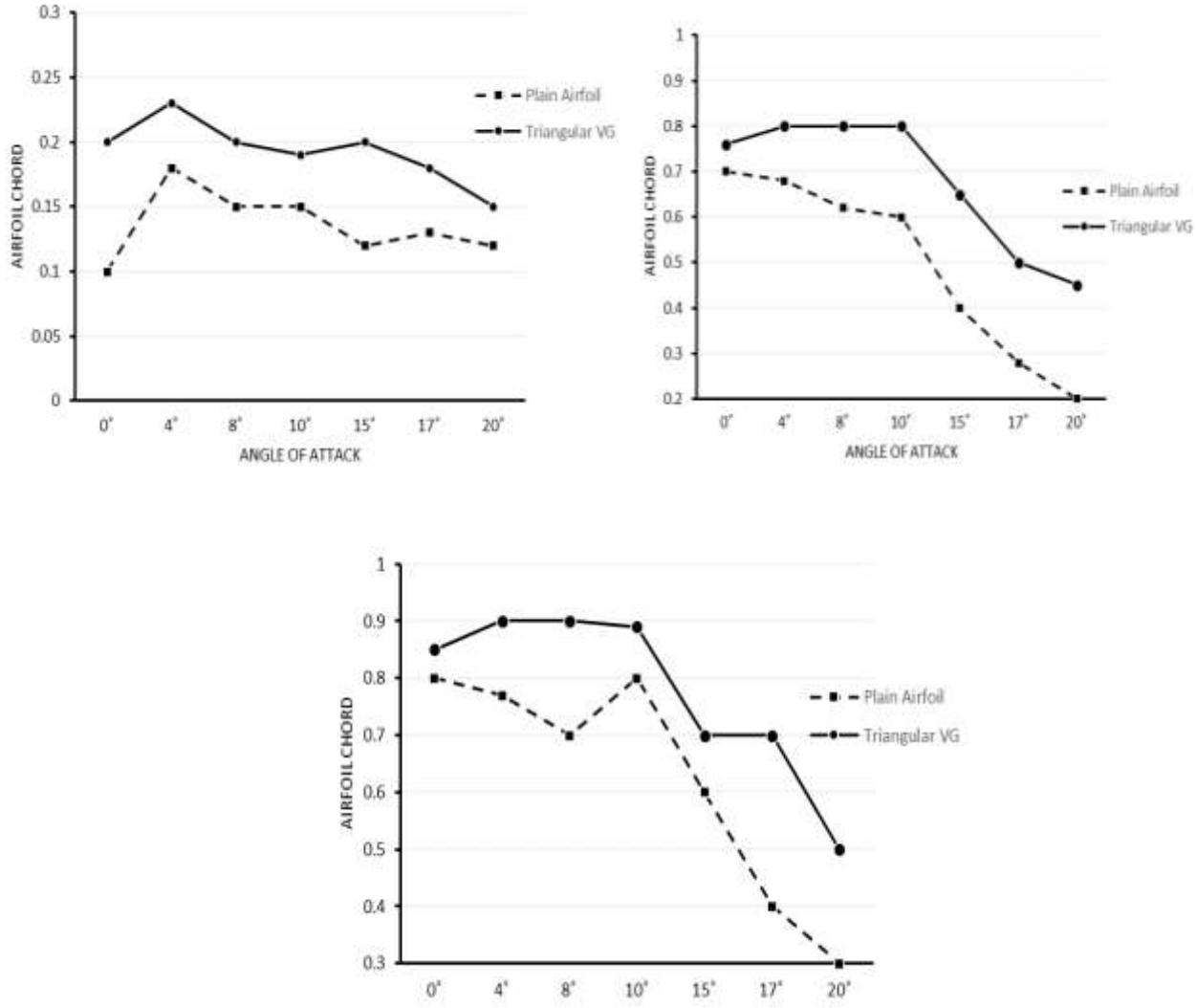

Figure 6. (a) Transition Point (b) Separation Point (c) Vortisitas Point

The addition of a vortex generator (VG) consistently results in a shift in the transition point as the angle of attack increases. As illustrated in Figure 6a, the transition flow observed in the experiment progresses from laminar to turbulent flow. These two flow regimes exhibit distinct characteristics: laminar flow is typically characterized by low velocity, irregularity, and a thinner boundary layer, whereas turbulent flow is faster, thicker, and exhibits more pronounced flow separation. Notably, the transition point increased by approximately 0.1 to 0.2 as the angle of attack increased from 0° to 20°. This effect can be attributed to the vortex generator's ability to expedite the transition from laminar to turbulent flow. In Figure 6b, the separation point accelerates as the angle of attack increases, particularly in the absence of a vortex generator. This accelerated separation occurs because the flow cannot maintain adherence to the surface in the absence of friction, resulting in earlier separation [18]. At a 20° angle of attack, for instance, the separation point occurs at approximately 0.2 without the vortex generator, but this point shifts to 0.4 when the vortex generator is present. This effect is particularly noticeable at higher angles of attack, where the vortex

DOI: https://doi.org/10.71225/jstn.v2i1.86

generator helps delay the onset of stall and increases the lift generated by the airfoil. Furthermore, the velocity of the smoke flow decreases with the distance traveled along the surface, and undirected flow exacerbates this effect. The separation flow continues until lift is lost, which is represented by the vorticity point. As shown in Figure 6c, the vorticity point shifts downstream with the addition of the vortex generator, thus delaying the stall point on the upper surface of the airfoil. As the angle of attack increases, the pressure coefficient rises, and the vortex flow moves further from the airfoil's upper surface, where it no longer contributes to lift or aerodynamic benefits. This emphasizes the importance of high-lift devices, such as vortex generators, in controlling airflow over the upper surface and delaying the rapid onset of stall at high angles of attack, thus enhancing aerodynamic performance and control authority, especially at low speeds. At the separation point, Figure 6b demonstrates that the presence of the vortex generator significantly delays the onset of flow separation at angles of 8°, 10°, and 15°, as indicated by the shift in the separation curve. The effect of the vortex generator is particularly pronounced at higher angles of attack, such as 15°, where lift is still maintained at approximately 0.1. In contrast, without the vortex generator, the airfoil typically loses lift at these higher angles. Additionally, the results show that placing the vortex generator at a 20% position relative to the leading edge significantly enhances lift at all angles of attack. As shown in Figure 6c, the vortices induced by the vortex generator move progressively farther from the airfoil's upper surface, further delaying the separation point. In the absence of the vortex generator, the vorticity point at a 20° angle of attack occurs at 0.3, while with the vortex generator, it occurs at 0.5, representing a shift of 0.2 along the surface. This finding underscores the significant impact of the vortex generator in improving flow stability, particularly at higher angles of attack [20] [22].

3.2 Smoke Flow Characteristics on Airfoil without Vortex Generator and using Triangular Vortex Generator

This experiment aims to visualize the transition of smoke flow from laminar to turbulent flow under varying angles of attack, with corresponding changes in transition and separation points influenced by the triangular vortex generator. The NACA 0012 airfoil is divided into 10% segments along its length, from the leading edge to the trailing edge. Key points on the airfoil are identified as follows: the stagnation point (Xp) is marked in green, the transition point (Xl) in yellow, the vorticity point (Xt) in blue, and the separation point (Xs) in red. The vortex generator is placed at 20% of the chord length from the leading edge.

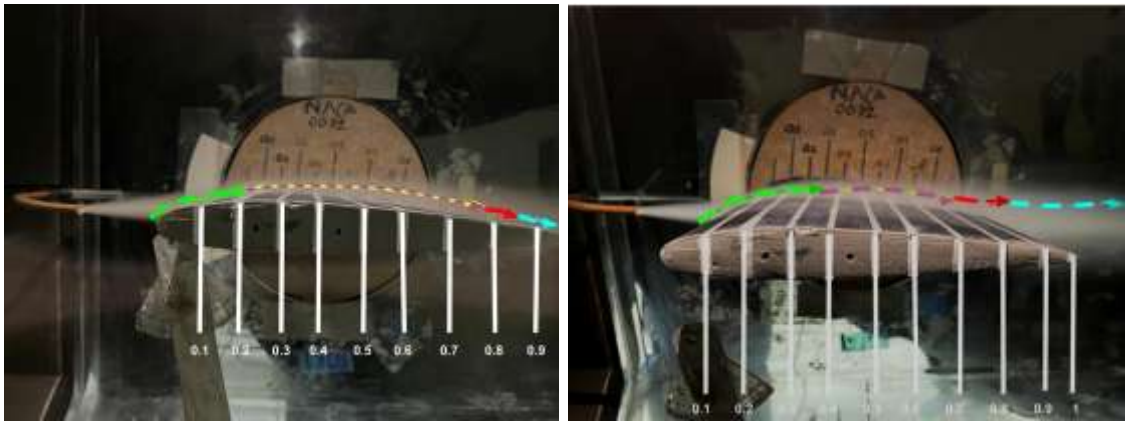

Figure 7. Speed 5 m/s (a) Plain Airfoil NACA 0012 α = 0˚ (b) Airfoil NACA 0012 with Triangular vortex generator α = 0˚

DOI: https://doi.org/10.71225/jstn.v2i1.86

For the airfoil without the vortex generator, the smoke flow transitions from laminar to turbulent between 0.2 and 0.75 of the chord length. Separation occurs between 0.7 and 0.8, with the vorticity point from 0.8 to the trailing edge. The flow appears thin due to the influence of laminar flow, which is characterized by an early separation point. With the addition of the triangular vortex generator, the transition occurs between 0.2 and 0.75, while the separation point shifts to 0.76. The vorticity point extends from 0.85 to the trailing edge.

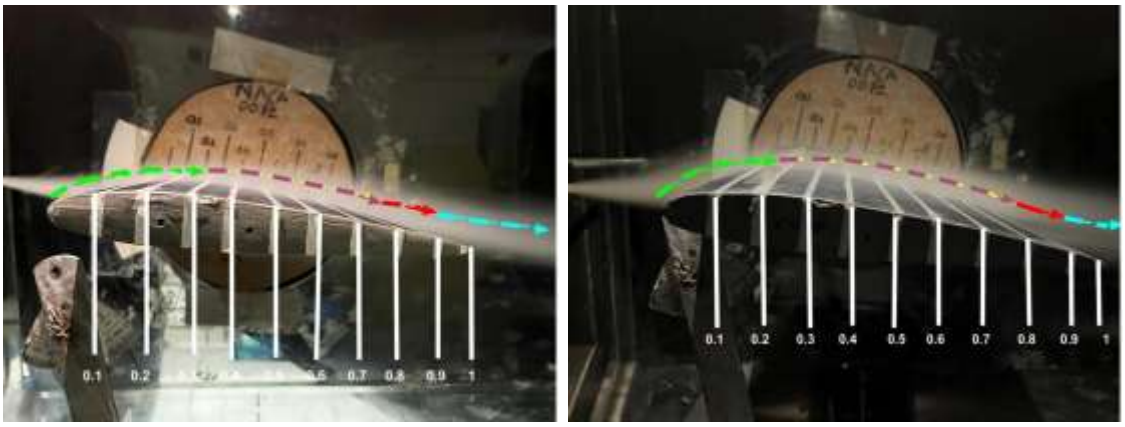

Figure 8. Speed 5 m/s (a) Plain Airfoil NACA 0012 α = 4˚ (b) Airfoil NACA 0012 with Triangular vortex generator α = 4˚

For the plain airfoil, the transition occurs between 0.18 and 0.7, with separation at 0.68 and vorticity starting at 0.77. The smoke flow dissipates without a distinct direction towards the trailing edge. In contrast, with the triangular vortex generator, the transition point occurs between 0.23 and 0.8, with separation at 0.8 and vorticity from 0.9 to the trailing edge.

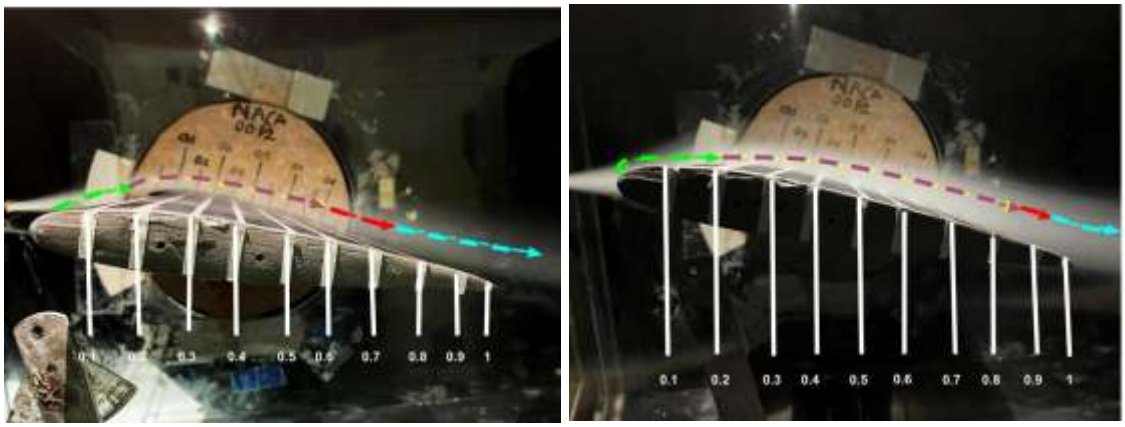

Figure 9. Speed 5 m/s (a) Plain Airfoil NACA 0012 α = 8˚ (b) Airfoil NACA 0012 with Triangular vortex generator α = 8˚

For the plain airfoil, the transition point is observed between 0.15 and 0.6, with the separation point between 0.6 and 0.7. With the vortex generator, the separation point moves to 0.85, and the vorticity point extends from 0.9 to the trailing edge, indicating the effectiveness of the vortex generator

DOI: https://doi.org/10.71225/jstn.v2i1.86

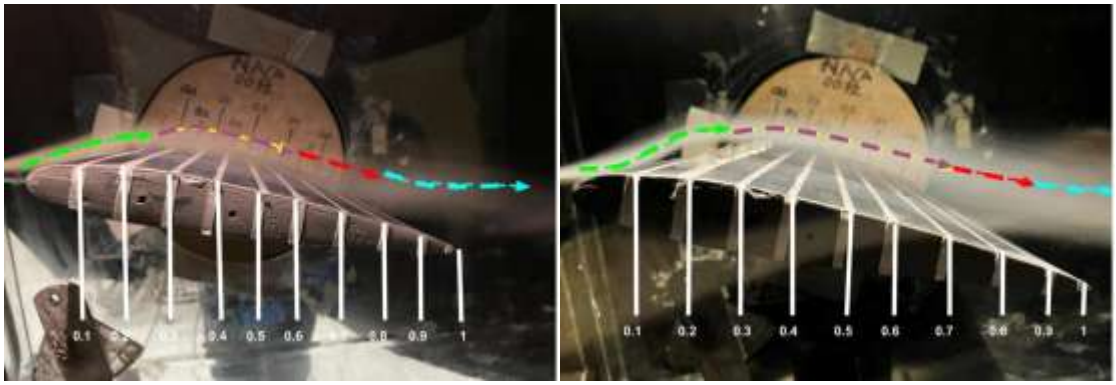

Figure 9. Speed 5 m/s (a) Plain Airfoil NACA 0012 α = 10˚ (b) Airfoil NACA 0012 with Triangular vortex generator α = 10˚

The transition point on the plain airfoil occurs between 0.15 and 0.6, with separation from 0.6 to 0.8. Vorticity starts at 0.8 and continues to the trailing edge. With the vortex generator, the transition point extends from 0.19 to 0.8, with separation at 0.9 and vorticity from 0.9 to the trailing edge.

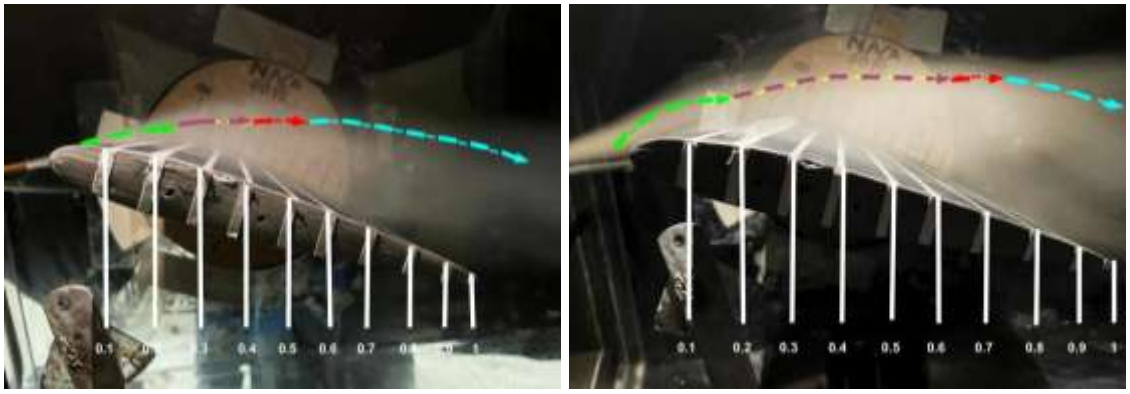

Figure 10. Speed 5 m/s (a) Plain Airfoil NACA 0012 α = 15˚ (b) Airfoil NACA 0012 with Triangular vortex generator α = 15˚

At this angle of attack, the flow has stalled, with the transition point occurring between 0.1 and 0.3. The separation point occurs from 0.4 to 0.6, and vorticity spans from 0.6 to the trailing edge. With the vortex generator, the transition point extends from 0.2 to 0.65, with separation occurring between 0.6 and 0.7. Vorticity spans from 0.7 to the trailing edge.

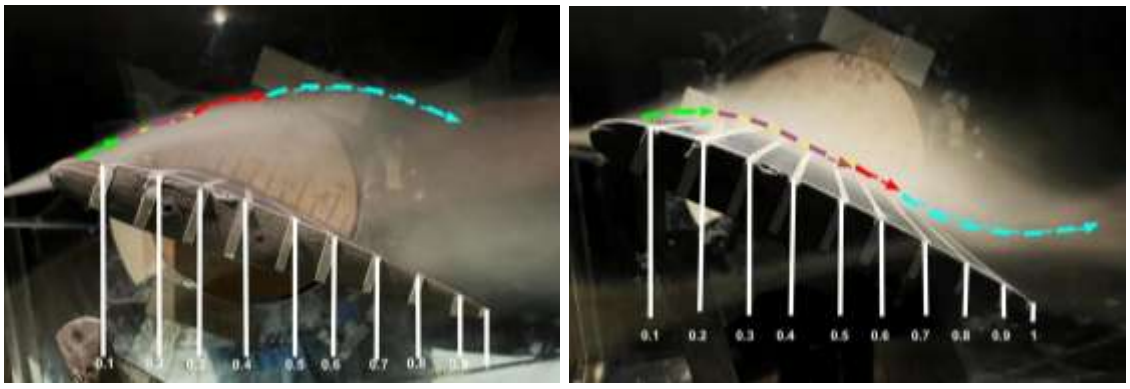

Figure 10. Speed 5 m/s (a) Plain Airfoil NACA 0012 α = 17˚ (b) Airfoil NACA 0012 with Triangular vortex generator α = 17˚

DOI: https://doi.org/10.71225/jstn.v2i1.86

At 17˚, the plain airfoil shows transition between 0.13 and 0.28, with separation occurring at 0.28. With the vortex generator, the transition point occurs from 0.18 to 0.5, with separation at 0.7.

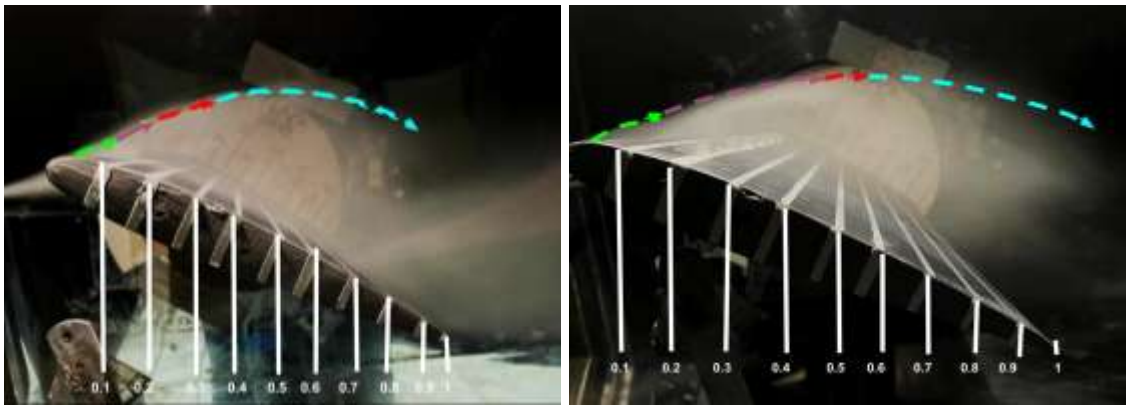

Figure 10. Speed 5 m/s (a) Plain Airfoil NACA 0012 α = 20˚ (b) Airfoil NACA 0012 with Triangular vortex generator α = 20˚

For the plain airfoil, a turbulent flow is observed with the transition point at 0.12, and separation occurs at 0.2. With the vortex generator, the transition point extends from 0.15 to 0.45, and the separation point is observed at 0.45, followed by irregular smoke flow to the trailing edge.

The experimental data gathered from the NACA 0012 airfoil, both with and without a triangular vortex generator, reveal significant differences in the airflow characteristics across various angles of attack. At a speed of 5 m/s and an angle of attack of 0˚, the airfoil without the vortex generator shows a transition from laminar to turbulent flow between 0.2 and 0.75 of the chord length, with separation occurring between 0.7 and 0.8. The addition of the triangular vortex generator shifts the separation point to 0.76 and extends the vorticity from 0.85 to the trailing edge. As the angle of attack increases to 4˚, the transition occurs between 0.18 and 0.7 for the plain airfoil, while the vortex generator moves the transition point from 0.23 to 0.8 and shifts the separation point to 0.8. At higher angles of attack, such as 8˚ and 10˚, the vortex generator continues to extend the separation point, from 0.85 to the trailing edge at 8˚ and from 0.9 to the trailing edge at 10˚. At angles of 15˚, 17˚, and 20˚, where the flow tends to stall without the vortex generator, the transition and separation points are significantly altered with the vortex generator, improving airflow stability by extending transition points and delaying separation. The vortex generator's effectiveness is particularly evident at higher angles of attack, where it helps maintain laminar flow for longer, reducing the risk of premature flow separation and enhancing the overall aerodynamic performance of the airfoil [23] [24].

The addition of the vortex generator significantly alters the airflow characteristics on the upper surface of the airfoil, particularly at higher angles of attack. The vortex generator helps to stabilize the airflow and delay separation, which would otherwise occur more rapidly at higher angles of attack. Laminar flow, characterized by low friction and drag coefficients, transitions into turbulent flow as the boundary layer thickness increases. The turbulence generated by the vortex generator helps to delay separation, reducing the risk of stalling and increasing the airfoil's performance [10] [15].

At an angle of attack of 15˚, for instance, without the vortex generator, the transition point occurs at 0.1, and separation occurs at 0.4. After the addition of the vortex generator, the separation point shifts further downstream to 0.65. Similar trends are observed at 17˚ and 20˚ angles of attack, where the vortex generator effectively delays separation and increases the overall stability of the airflow. This leads to enhanced aerodynamic performance, especially at higher angles of attack where flow separation is a concern [8] [10].

DOI: https://doi.org/10.71225/jstn.v2i1.86

In conclusion, the triangular vortex generator proves effective in improving the aerodynamic characteristics of the airfoil, particularly by delaying flow separation and enhancing the stability of the airflow at high angles of attack. The results demonstrate the potential of vortex generators as a high-lift device for improving the performance of airfoils under various flight conditions.

4. Conclusion

The purpose of this study was to compare the airflow characteristics of a plain NACA 0012 airfoil and one equipped with a triangular vortex generator (VG) placed 20% from the leading edge, under a freestream speed of 5 m/s. The key findings include that the addition of the VG improved airflow performance by facilitating the transition from laminar to turbulent flow, reducing flow separation, and increasing the speed of the smoke stream. Specifically, at angles of attack of 8˚ and 10˚, the VG maintained a transition point, while at 0˚ and 15˚, the transition point was longer due to frictional effects on the surface. Moreover, the vortex generator was effective at maintaining lift even at higher angles of attack (15˚, 17˚, and 20˚), where the airfoil had stalled, with the coefficient of lift (CL) increasing from 0˚ onward. Analysis of the variation in angles of attack showed that the vortex generator mitigated flow separation and turbulence, enhancing aerodynamic performance across the tested angles. However, the study has some limitations, such as the limited scope of VG placement and freestream speed. Future research should explore different VG placements, higher speeds, and other airfoil designs to further understand the impact of vortex generators on aerodynamic efficiency.

Acknowledgments

Thank you our sincere gratitude to the lecturers of Department of Maintenance Engineering Politeknik Penerbangan Surabaya for their invaluable guidance and support throughout this research.

References

[1] N.N. Gavrilović, B.P. Rašuo, G.S. Dulikravich, and V.B. Parezanović, “Commercial aircraft performance improvement using winglets,” FME Transactions, vol. 43, no. 1, pp. 1–8, 2015.

[2] S. Gudmundsson, General Aviation Aircraft Design : Applied Methods, First edit. New York: Butterworth-Heinemann is an imprint of Elsevier, 2013.

[3] Y.H. Chen, J.J. Miau, Y.P. Chen, and Y.R. Chen, “Blunt leading-edge effect on spanwise-varying leading-edge contours of an UCAV configuration,” Journal of Fluid Science and Technology, vol. 18, no. 1, pp. 1–11, 2023.

[4] D. Raffaele, T.P. Waters, E. Rustighi, and U. Kingdom, “Wave propagation in an aircraft wing slat for de-icing purposes,” 3rd Euro-Mediterranean Conference on Structural Dynamics and Vibroacoustics. Università degli Studi di Napoli, pp. 17–20, 2020.

[5] X. Xu, T. Wang, Y. Fu, Y. Zhang, and G. Chen, “Numerical research of an ice accretion delay method by the bio-inspired leading edge,” Aerospace, vol. 9, no. 12, p. 774, 2022.

[6] E.S. Elumalai, A.G. Agarwal, B.K. Singh and G. Krishnaveni, “Numerical simulation of bird strike effect on a composite wing leading edge,” Test Engineering and Management, vol. 83, pp. 7472–7481, 2020.

[7] J. Wang, J. Wang, and K.C. Kim, “Wake/shear layer interaction for low-Reynolds-number flow over multi-element airfoil,”Experiments in Fluids, vol. 60, pp. 1-24, 2019.

DOI: https://doi.org/10.71225/jstn.v2i1.86

[8] J. Yu and B. Mi, “A new flow control method of slat-grid channel-coupled configuration on high-lift device,” Applied Sciences, vol. 13, no. 6, p. 3488 2023.
[9] A.P. Markesteijn, H.K. Jawahar, S.A. Karabasov, and M. Azarpeyvand, “GPU CABARET Solutions for 30P30N three-element high-lift airfoil with slat modification,” in 2021 AIAA AVIATION Forum and Exposition, American Institute of Aeronautics and Astronautics, p. 2115, 2021.
[10] M.P.J. Sanders, L.D. de Santana, and C.H. Venner, “The sweep angle effect on slat noise characteristics of the 30p30n high- lift model in an open-jet wind tunnel,” AIAA Aviation 2020 Forum, p. 2557, 2020.
[11] R. Wei, Y. Liu, X. Li, and H. Zhang, “Experimental study on the oscillation of the shear layer of the slat cavity for 30P30N multi-element high-lift airfoil,” AIAA AVIATION 2023 Forum, p. 4482, 2023.
[12] F.L. dos Santos, K. Venner, and L.D. de Santana, “Turbulence distortion effects for leading-edge noise prediction,” 28th International Congress on Sound and Vibration, ICSV 2022, pp. 1–8, 2022.
[13] G. Kuntumalla, Y. Meng, M. Rajagopal, R. Toro, H. Zhao, HC. Chang et al., “Joining techniques for novel metal polymer hybrid heat exchangers,” ASME International Mechanical Engineering Congress and Exposition, vol. 59384, p. V02BT02A018, 2019.
[14] P. Singh, L. Neuhaus, O. Huxdorf, J. Riemenschneider, J. Wild, J. Peinke, and M. Hölling, “Experimental investigation of an active slat for airfoil load alleviation,” Journal of Renewable and Sustainable Energy, vol. 13, no. 4, p. 043304, 2021.
[15] S. Antoniou, S. Kapsalis, P. Panagiotou, and K. Yakinthos, “Parametric investigation of leading-edge slats on a blended-wing- body UAV using the Taguchi method,” Aerospace, vol. 10, no. 8, p. 720, 2023.
[16] L.W. Traub and M.P. Kaula, “Effect of leading-edge slats at low Reynolds numbers,” Aerospace, vol. 3, no. 4, p. 39, 2016.
[17] S.P. Setyo Hariyadi, B. Junipitoyo, N. Pambudiyatno, Sutardi, and W.A. Widodo, “Aerodynamic characteristics of fluid flow on multiple-element wing airfoil Naca 43018 with leading-edge slat and plain flap,” Journal of Engineering Science and Technology, vol. 18, no. 1, pp. 36–50, 2023.
[18] H. Lv, X. Zhang, and J. Kuang, “Numerical simulation of aerodynamic characteristics of multi-element wing with variable flap,” Journal of Physics: Conference Series, vol. 916, no. 1, p. 012005, 2017.
[19] S.P.S. Hariyadi, N. Pambudiyatno, Sutardi, and P.F. Dyan, “Aerodynamic characteristics of the wing airfoil NACA 43018 in take off conditions with slat clearance and flap deflection,” in Recent Advances in Mechanical Engineering: Select Proceedings of ICOME 2021. Singapore: Springer Nature Singapore, pp. 220–229, 2022.
[20] S.H.S. Putro, S. Sutardi, W.A. Widodo, N. Pambudiyatno, and I. Sonhaji, “Effect of leading-edge gap size on multiple-element wing NACA 43018,” International Review of Aerospace Engineering, vol. 15, no. 12, pp. 30–40, 2022.
[21] N.J. Mulvany, L. Chen, J.Y. Tu, and B. Anderson, “Steady-state evaluation of two-equation RANS (Reynolds-Averaged Navier-Stokes) turbulence models for high-Reynolds number hydrodynamic flow simulations,” Department of Defence, Australian Government, DSTO Platform Sciences Laboratory, Australia, 2004.
[22] S. Tobing, “Lift generation of an elliptical airfoil at a Reynolds number of 1000,” International Journal of Automotive and Mechanical Engineering, vol. 16, no. 2, pp. 6738–6752, 2019.

DOI: https://doi.org/10.71225/jstn.v2i1.86

[23] S. Jamei, A. Maimun, N. Azwadi, M.M. Tofa, S. Mansor, and A. Priyanto, “Ground viscous effect on 3D flow structure of a compound wing-in-ground effect,” International Journal of Automotive and Mechanical Engineering, vol. 9, pp. 1550–1563, 2014.
[24] S.P. Setyo Hariyadi, Sutardi, W.A. Widodo, and M.A. Mustaghfirin, “Aerodynamics analysis of the wingtip fence effect on UAV wing,” International Review of Mechanical Engineering, vol. 12, no. 10, pp. 837–846, 2018.
[25] S.S.P. Hariyadi, B. Junipitoyo, W.A. Widodo, I. Sonhaji and F.D. Pertiwi, “Numerical simulation using slats, slots, and flaps in steady flight conditions,” Advances in Science and Technology, vol. 112, pp. 22–31, 2022.
[26] Z.T. Dayanti, S. Hariyadi, and I.S. Rifdian, “Experimental study of fluid flow characteristics in wing airfoil NACA 43018 with parabolic vortex generator using oil flow visualization,” in Proceedings of the International Conference on Advance Transportation, Engineering, and Applied Science (ICATEAS 2022), Surabaya: Atlantis Press International BV, pp. 52–69, 2023.
[27] Y. Fujita and M. Iima, “Aerodynamic performance of dragonfly wing model that starts impulsively: how vortex motion works,” Journal of Fluid Science and Technology, vol. 18, no. 1, p. JFST0013, 2023.
[28] M. Hojaji, M.R. Soufivand, and R. Lavimi, “An experimental comparison between wing root and wingtip corrugation patterns of dragonfly wing at ultra-low Reynolds number and high angles of attack,” Journal of Applied and Computational Mechanics, vol. 8, no. 4, pp. 1176–1185, 2022.
[29] K.A. Kasim, P. Segard, S. Mat, S. Mansor, M.N. Dahalan, N.A.R.N. Mohd et al., “Effects of the propeller advance ratio on delta wing UAV leading edge vortex,” International Journal of Automotive and Mechanical Engineering, vol. 16, no. 3, pp. 6958–6970, 2019.
[30] I. Madan, N. Tajudin, M. Said, S. Mat, N. Othman, M.A. Wahid et al., “Influence of active flow control on blunt-edged VFE-2 delta wing model,” International Journal of Automotive and Mechanical Engineering, vol. 18, no. 1, pp. 8411–8422, 2021.
[31] M. Said, M. Imai, S. Mat, M.N. Dahalan, S. Mansor, M.N.M. Nasir et al., “Tuft flow visualisation on UTM-LST VFE-2 delta wing model configuration at high angle of attacks,” International Journal of Automotive and Mechanical Engineering, vol. 17, no. 3, pp. 8214–8223, 2020.
[32] S. Hariyadi Suranto Putro, B. Junipitoyo, N. Pambudiyatno, Sutardi, and W. Aries Widodo, “Aerodynamic characteristics of fluid flow on multiple-element wing airfoil NACA 43018 with leading-edge slat and plain flap,” Journal of Engineering Science and Technology, vol. 1, no. 1, pp. 36–50, 2023.
[33] D.G. Urbano, G. Noventa, A. Ghidoni, and A.M. Lezzi, “A semi-empirical fluid dynamic model of a vacuum microgripper based on CFD analysis,” Applied Sciences, vol. 11, no. 16, p. 7482, 2021.
[34] V.S. Dinh, C.T. Dinh, and V.S. Pham, “Numerical study on aerodynamic characteristics of the grid fins with different grid patterns,” Physics of Fluids, vol. 35, no. 12, p. 123117, 2023.
[35] S.G. Kontogiannis, D.E. Mazarakos, and V. Kostopoulos, “ATLAS IV wing aerodynamic design: From conceptual approach to detailed optimization,” Aerospace Science and Technology, vol. 56, pp. 135–147, 2016.
[36] A. Roy, A.K. Mallik, and T.P. Sarma, “A study of model separation flow behavior at high angles of attack aerodynamics,”Journal of Applied and Computational Mechanics, vol. 4, no. 4, pp. 318–330, 2018.

DOI: https://doi.org/10.71225/jstn.v2i1.86